Supplementary figures and table for

Structural insights into the mechanism of phosphate recognition and transport by human XPR1

Wenhui Zhang[1,#], Yanke Chen[2,#], Zeyuan Guan[1,#], Zhangmeng Du[1], Meng Cheng[1], Jie Zhang[1], Jiaqi Zuo[1], Peng Cheng[1], Qiang Wang[1], Yanjun Liu[1], Delin Zhang[1], Ping Yin[1], Zhu Liu[1*]

[1]National Key Laboratory of Crop Genetic Improvement, Hubei Hongshan Laboratory, Huazhong Agricultural University, Wuhan 430070, China.

[2]College of Biomedicine and Health, Huazhong Agricultural University, Wuhan 430070, China.

[#]These authors contributed equally to this work.

[*]Corresponding author: liuzhu@hzau.edu.cn (Z. L.).

This PDF file includes:

Supplementary Figs. 1-6

Supplementary Table 1

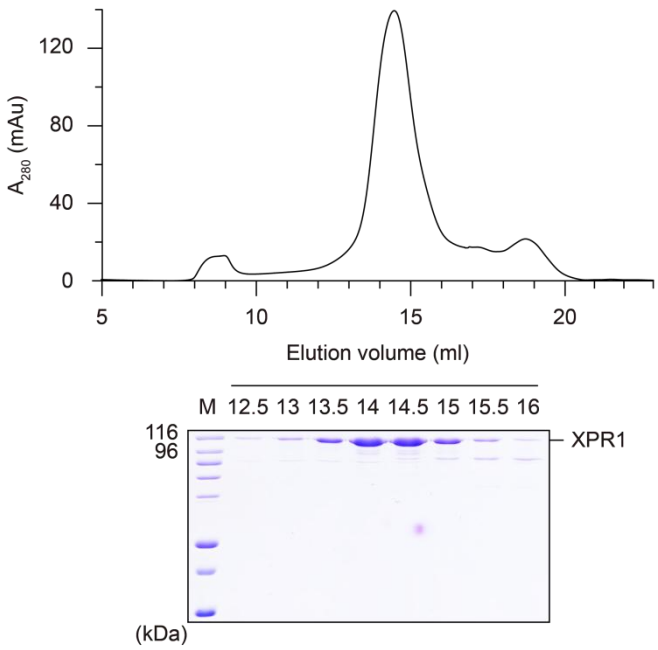

Supplementary Fig. 1. XPR1 purification for Cryo-EM analysis. Representative size-exclusion chromatography (SEC) purification of XPR1 in the presence of $InsP_6$. Fractions of XPR1 at 14-14.5 ml elution volume were collected and concentrated for preparing Cryo-EM grids.

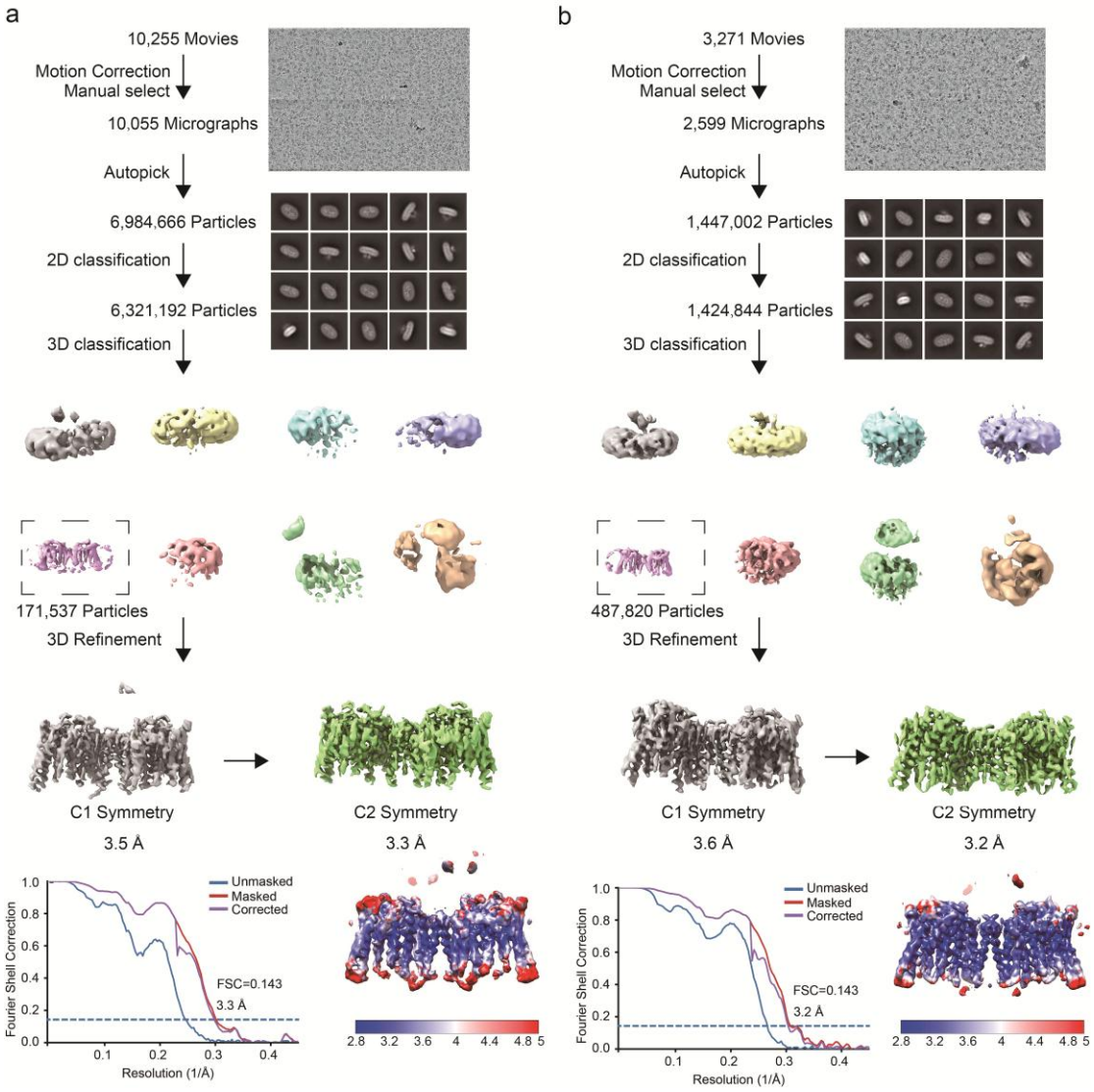

Supplementary Fig. 2. Cryo-EM structural analysis of XPR1. Flow chart for EM data processing of the wild-type XPR1 (**a**) and mutant XPR1 (**b**).

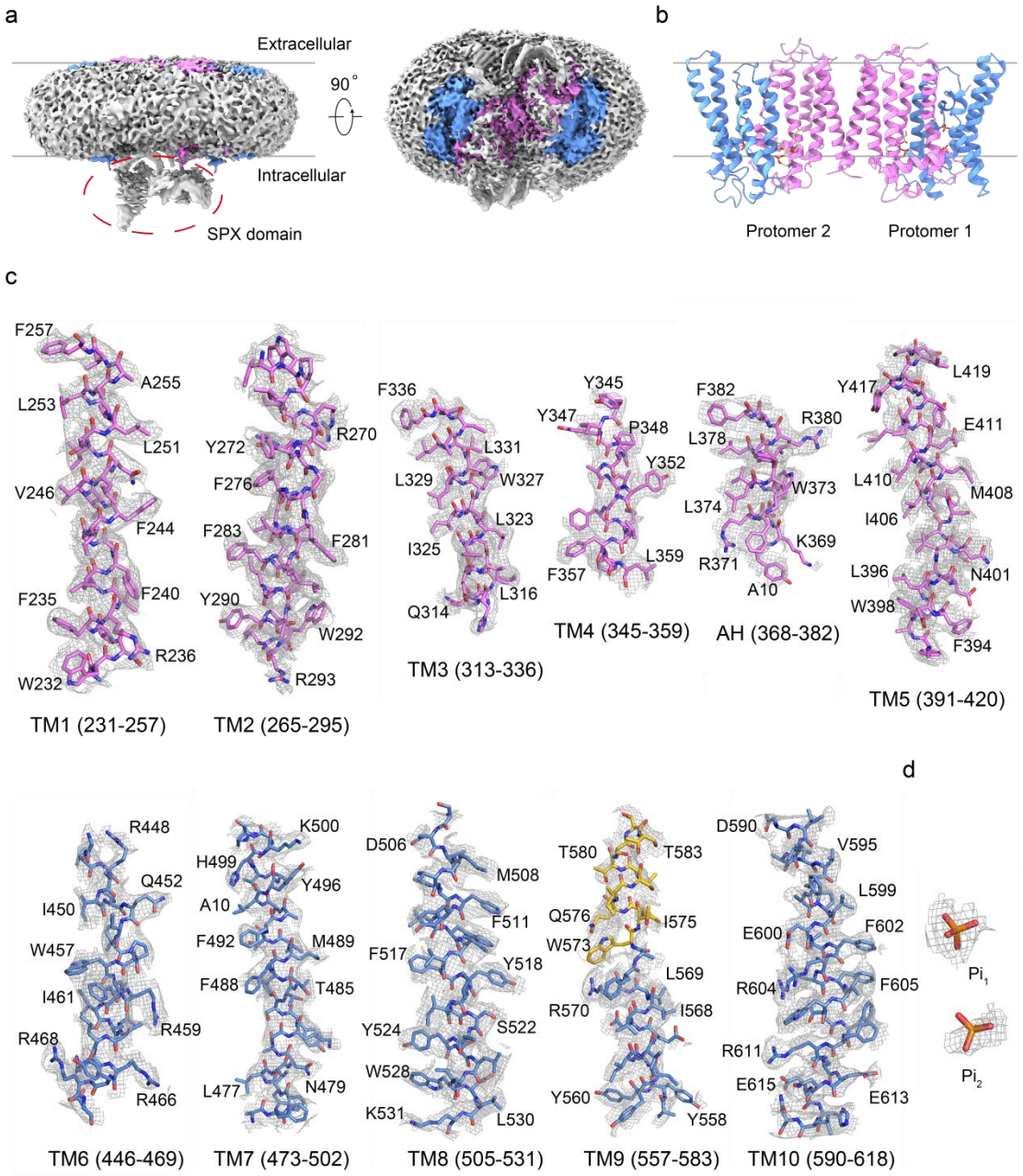

Supplementary Fig. 3. EM densities and representative elements of XPR1. a EM density map with low display threshold reveals the signals of the cytoplasmic SPX domain and detergent. The transmembrane domain of XPR1 is colored in the same scheme as Fig. 1a in the main text. XPR1 presents as a dimer in the EM map. **b** Cartoon representation of the resolved dimeric transmembrane domain of XPR1. The two protomers adopt similar structure with an overall RMSD of 0.41. Protomer 1 (chain A) is used for further analysis and discussion in this manuscript. Two phosphate ions present in both protomers. Additionally, lipid-like densities have been modeled using phosphatidylcholine molecules. Phosphate and phosphatidylcholine are shown as sticks. **c** EM density maps for the indicated transmembrane α-helices and **d** phosphate ions, respectively. All the densities are contoured at 5.5 σ and visualized using PyMol 2.4.1.

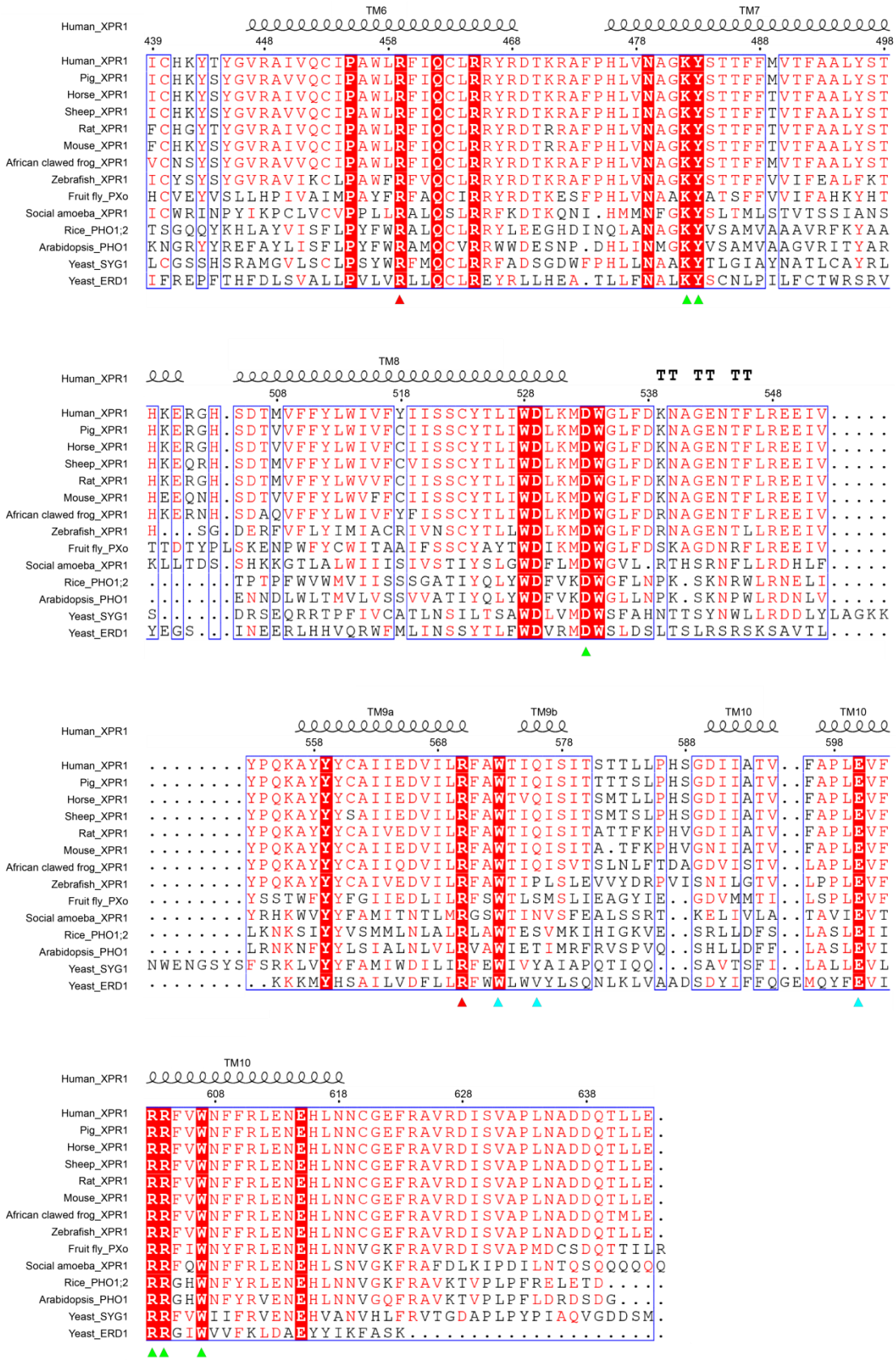

Supplementary Fig. 4. Sequence alignment of EXS domain-containing proteins. The sequence of EXS domain from human XPR1 is aligned with other orthologues. Structure-based alignment was performed by ESPript (3.0). The sequence identity is

indicated by white letters against a red background, and the sequence of a similarity over 90% is indicated by red letters. The secondary elements of EXS domain from human XPR1 are labeled at the top of the alignment. The residues responsible for Pi_1 and Pi_2 binding are indicated with cyan and green triangles at the bottom of the alignment, respectively. The sites (R459 and R570) where mutations were found in PFBC families are indicated by red triangles.

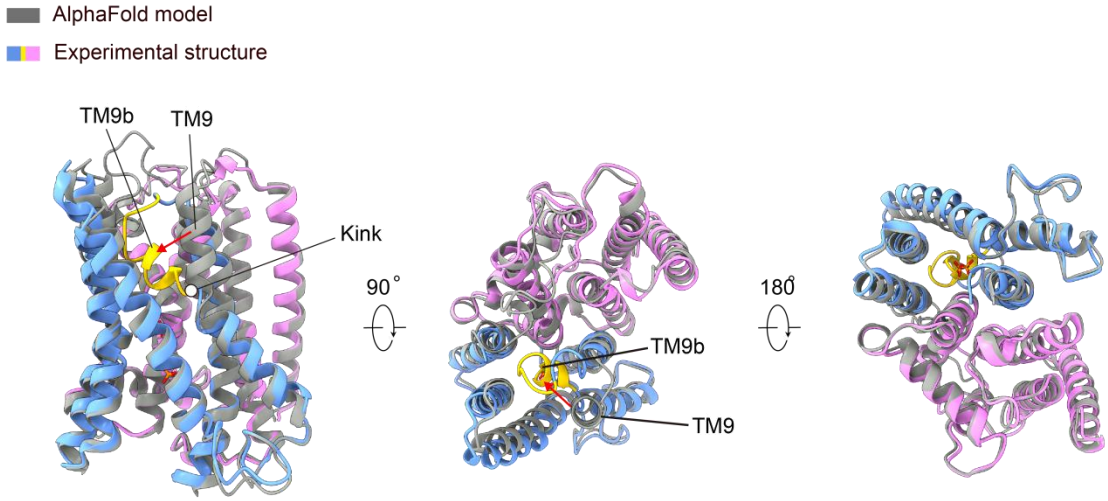

Supplementary Fig. 5. Comparison between the experimental structure of XPR1 transmembrane domian bound to phosphate ions and the unbound state model predicted by AlphaFold. The experimental structure is colored in the same scheme as Fig. 1a in the main text. The AlphaFold model (AF-Q9UBH6-F1) is superposed and colored in gray.

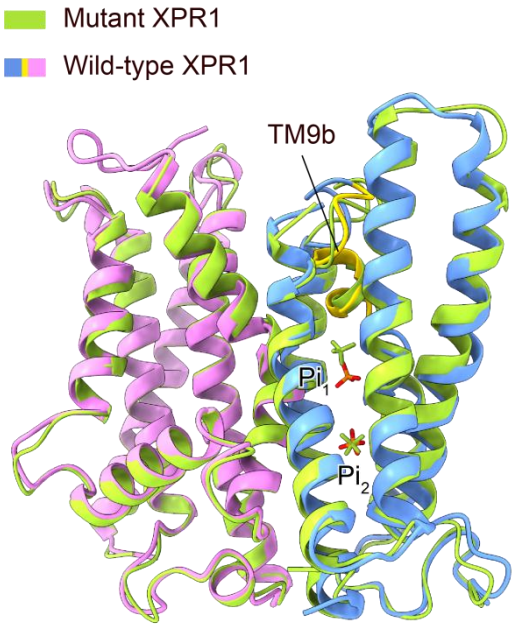

Supplementary Fig. 6. Structure comparison between the transmembrane domain of wild-type and mutant XPR1. The wild-type structure is colored in the same scheme as Fig. 1a in the main text. The mutant structure is superposed and colored in light green.

Supplementary Table 1.

Cryo-EM data collection, refinement and validation statistics

	Wild-type XPR1 (EMD-37205) (PDB 8KFM)	Mutant XPR1 (EMD-37239) (PDB 8KHB)
Data collection and processing		
Magnification	81,000	81,000
Voltage (kV)	300	300
Electron exposure (e^{-}/Å^2)	50	50
Defocus range (μm)	-1.2~-2.2	-1.2~-2.2
Pixel size (Å)	1.07	1.07
Symmetry imposed	C2	C2
Initial particle images (no.)	6,984,666	1,447,002
Final particle images (no.)	171,537	487,820
Map resolution (Å)	3.3	3.2
FSC threshold	0.143	0.143
Map resolution range (Å)	2.8~5.0	2.8~5.0
Refinement		
Initial model used	Alphafold2	8KFM
Model resolution (Å)	3.22/3.56	3.16/3.34
FSC threshold	0.143/0.5	0.143/0.5
Map sharpening *B* factor (Å^2)	146.4	174.5
Model composition		
Non-hydrogen atoms	6,372	6,222
Protein residues	754	739
Ligands	6	6
B factors (Å^2)		
Protein	79.67	70.51
Ligand	65.41	55.66
R.m.s. deviations		
Bond lengths (Å)	0.004	0.015
Bond angles (°)	0.629	1.324
Validation		
MolProbity score	1.85	1.93
Clashscore	14.36	12.79
Poor rotamers (%)	0.6	0.92
Ramachandran plot		
Favored (%)	96.92	95.49
Allowed (%)	3.08	4.51
Disallowed (%)	0	0